Chen *et al.*
BMC Complementary Medicine and Therapies (2022) 22:144
https://doi.org/10.1186/s12906-022-03609-x

BMC Complementary Medicine and Therapies

RESEARCH

Open Access

Photoprotective effects of *Sargassum thunbergii* on ultraviolet B-induced mouse L929 fibroblasts and zebrafish

Bei Chen[1†], Honghong Chen[2,3†], Haidong Qu[4], Kun Qiao[1], Min Xu[1], Jingna Wu[5], Yongchang Su[1], Yan Shi[2], Zhiyu Liu[1*] and Qin Wang[2*]

Abstract

Background: Chronic exposure to ultraviolet B (UVB) causes a series of adverse skin reactions, such as erythema, sunburn, photoaging, and cancer, by altering signaling pathways related to inflammation, oxidative stress, and DNA damage. Marine algae have abundant amounts and varieties of bioactive compounds that possess antioxidant and anti-inflammatory properties. Thus, the objective of this study was to investigate the photoprotective effects of an ethanol extract of *Sargassum thunbergii*.

Methods: *Sargassum thunbergii* phenolic-rich extract (STPE) was prepared, and its activity against UVB damage was evaluated using L929 fibroblast cells and zebrafish. STPE was extracted and purified by 40% ethanol and macroporous resin XDA-7. Reactive oxygen species (ROS) and antioxidant markers, such as superoxide dismutase (SOD), catalase (CAT) activities, and malondialdehyde (MDA) content were analyzed. The effect of STPE on UVB-induced inflammation was determined by inflammatory cytokine gene and protein expression. The expression of signaling molecules in the Nuclear Factor KappaB (NF-κB) pathway was determined by western blotting. DNA condensation was analyzed and visualized by Hoechst 33342 staining. In vivo evaluation was performed by tail fin area and ROS measurement using the zebrafish model.

Results: The total polyphenol content of STPE was 72%. STPE reduced ROS content in L929 cells, improved SOD and CAT activities, and significantly reduced MDA content, thereby effectively alleviating UVB radiation-induced oxidative damage. STPE inhibited the mRNA and protein expression of TNF-α, IL-6, and IL-1α. STPE reversed DNA condensation at concentrations of 20 and 40 μg/mL compared with the UVB control. Moreover, STPE inhibited NF-κB signaling pathway activation and alleviated DNA agglutination in L929 cells after UVB irradiation. Additionally, 1.67 μg/mL STPE significantly increased the tail fin area in zebrafish, and 0.8–1.6 μg/mL STPE effectively eliminated excessive ROS after UVB radiation.

†Bei Chen and Honghong Chen contributed equally to this work.

*Correspondence: 13906008638@163.com; qwang@xmu.edu.cn

[1] Fisheries Research Institute of Fujian, Key Laboratory of Cultivation and High-value Utilization of Marine Organisms in Fujian Province, No. 7, Haishan Road, Huli District, Xiamen 361013, Fujian, China
[2] School of Life Sciences, Xiamen University, South Xiangan Road, Xiang'an District, Xiamen 361102, Fujian, China
Full list of author information is available at the end of the article

Conclusions: STPE inhibited UVB-induced oxidative stress, inflammatory cytokine expression, and DNA condensation via the downregulation of the NF-κB signaling pathway, suggesting that it prevents UVB-induced photodamage, and has potential for clinical development for skin disease treatment.

Keywords: *Sargassum thunbergii*, Ultraviolet B, Photoprotective, L929 fibroblast, Zebrafish

Background

Among the types of ultraviolet (UV) rays that are not absorbed by the ozone layer, ultraviolet B (UVB) (wavelength 280–315 nm) is a major environmental risk factor for the pathogenesis of skin damage [1]. UVB delivers more energy into the skin than UVA (320–400 nm). Many skin diseases, such as cancer, photoaging, sunburn, and pigmentation, are closely associated with UVB exposure. Owing to its short wavelength, UVB is mainly absorbed in the epidermis; however, it can also penetrate this skin layer to reach the dermis and affect the physiological functions of fibroblasts [2]. Studies on UVB-irradiated skin or dermal fibroblasts have mainly focused on DNA mutations [3], inflammation [4], and photoaging [1, 5].

Marine phenolic compounds exhibit a wide range of physiological properties, including antioxidant, anti-inflammatory, anti-tumor, and anti-microbial properties [6, 7]. Recently, the UV protection activity of marine polyphenols has been intensively focused upon owing to the growing demand for anti-aging, anti-allergic, and whitening natural products in the skin health industry. Fucodiphlorethol G extracted from *Ecklonia cava* increases the viability of human keratinized cells exposed to UVB radiation by absorbing UVB, removing intracellular reactive oxygen species (ROS), and reducing 8-isoprostane generation and DNA fragmentation [8]. The phlorotannin fucofuroeckol-A, derived from *Ecklonia stolonifera*, demonstrates protective effects against UVB-induced allergic reactions in RBL-2H3 mast cells by decreasing histamine release, increasing intracellular Ca^{2+}, inhibiting IL-1β and TNF-α production, and scavenging ROS [9]. Diphlorethohydroxycarmalol extracted from *Ishige okamurae* exhibits strong protective properties against UVB radiation via reducing intracellular ROS levels, reducing damaged DNA tail length, and causing morphological changes in fibroblasts [10].

In the last decades, marine algae have been an important source of natural products to find new compounds with pharmacological and nutraceutical properties. *Sargassum thunbergii,* an economically important brown algae located on China and Japan seas, contains many bioactive compounds, such as indole derivatives, indolediketopiperazine alkaloids, quinone derivatives, polyphenols, and polysaccharides [11]. *S. thunbergii* lives in the intertidal zone undergoing multiple changes due to tidal changes, including high solar irradiances, desiccation, changes in salinity, and temperature. Therefore, we speculated that phenolic compounds from *S. thunbergii* might possess UV protective activity. However, to our knowledge, the photoprotective activity of *S. thunbergii* was unreported previously.

The mouse L929 fibroblast cell line is reportedly an effective in vitro screening test system for the phototoxicity assessment of drugs/chemicals [12]. Zebrafish (*Danio rerio*) are increasingly being considered as a model system for evaluating the efficacy of UVB protective compounds against fin damage and ROS generation [13, 14]. In this study, we established a UVB-exposed L929 cell and zebrafish photodamage model to study the UVB photoprotective activity of *S. thunbergii* phenolic-rich extract (STPE).

Methods

Reagents

A PierceTM BCA Protein Assay Kit, RPMI1640 medium, DPBS/MODIFIED, Trypsin-EDTA Solution, fetal bovine serum, and dual antibodies were purchased from Thermo Fisher Scientific (Waltham, MA, USA). A CellTiter 96 Aqueous Non-Radioactive Cell Proliferation Assay (MTS) kit was obtained from Promega (Madison, WI, USA) and phenazine methosulfate was purchased from Sigma-Aldrich (St. Louis, MO, USA). High Efficiency RIPA tissue/cell rapid lysis solution was acquired from Beijing Solarbio Science & Technology Co., Ltd. (Beijing, China). All antibodies were purchased from Abcam (Cambridge, MA, USA) or Cell Signaling Technology (Beverly, MA, USA) as follows: Nuclear Factor KappaB (NF-κB) p65 (D14E12) XP Rabbit mAb (#8242, dilution 1/1000), p-NF-κB p65 (Ser536) (93H1) rabbit mAb (#3033, dilution 1/1000), anti-IκBα antibody (ab32518, dilution 1/1000), anti-SDHA antibody (ab137040, dilution 1/1000), and anti-Lamin B antibody (ab133741, dilution 1/1000).

Phenolic compound extraction and purification

The material used in the preparation of the *S. thunbergii* phenolic-rich extract was obtained from the coastal reefs in Dongtou Island, Zhejiang Province, China. The algal handling procedures in this study comply with local and national regulations. The Committee for Conservation of Aquatic Germplasm, from the Mariculture Research Institute of Zhejiang, China, approved these

experiments. The wild type *S. thunbergii* algae was identified by Fujian Marine and Fisheries Judicial Expertise Center. A voucher specimen (ST20190402) was deposited at the Mariculture Research Institute of Zhejiang, China. Fresh *S. thunbergii* was delivered to Xiamen via cold chain logistics, followed by washing and freeze-drying. Dried *S. thunbergii* was crushed and powdered using a grinding mill. After 100-mesh screening, the powder was immersed in 40% (v/v) ethanol-water solution (solid to liquid ratio 1:15) for 60 min at 70 °C. After a double extraction, the extract was filtered using a Buchner funnel under vacuum. The supernatants were centrifuged at 12000 rpm for 30 min and concentrated to remove ethanol using a rotary evaporator (Buchi, Flawil, Switzerland). The crude *S. thunbergii* extract was further purified to obtain the STPE.

To purify the STPE, an XDA-7 macroporous resin (Sunresin Park, Xi'an, China) was used. Prior to use, the resin was activated by soaking with 95% ethanol for 24 h and subsequently washing thoroughly with deionized water. The resin was successively treated with 5% HCl and 4% NaOH solutions to remove potential monomers and porogenic agents trapped inside the pores during the synthesis process.

The crude extract was centrifuged at 12000 rpm for 30 min and filtered using a 0.45 μM filter. Subsequently, the extract was purified using a polystyrene column (Ø: 10 mm; h: 300 mm) packed with XDA-7 resin. For polyphenol adsorption, 3.2 mg/mL crude extract was passed through the resin at a flow rate of 1 mL/min. The loaded resin was washed with 3 BV deionized water prior to desorption. Desorption of phenolic compounds from the loaded XDA-7 macroporous resin was performed using 60% (v/v) ethanol solutions at a rate of 2 mL/min. The eluent was collected and concentrated under reduced pressure in a rotary evaporator. Finally, the purified extracts were stored at − 80 °C until further analysis.

The total polyphenol content was determined using the colorimetric Folin–Ciocalteu method with some modifications [15]. Gallic acid was used as a standard phenolic compound. One milliliter of extract solution contained 1 mg extract diluted with distilled water. Five milliliter of Folin-Ciocalteu reagent (10%) was added and the content was mixed thoroughly. After 3–8 min, 4 mL of 7.5% Na_2CO_3 was added and the mixture was allowed to stand for 1 h with occasional shaking. The absorbance was measured at 765 nm.

Cell culture and treatment

Murine L929 fibroblasts were grown in Dulbecco's modified eagle medium supplemented with 10% (v/v) heat-inactivated fetal bovine serum (FBS) and 1% (v/v) penicillin/streptomycin at 37 °C and 5% CO_2. Depending on the experiment, the cells were seeded in 96-well plates (1×10^5 cells/mL), 24-well plates (1×10^5 cells/mL), 6-well plates (1.5×10^5 cells/mL), or 60 mm culture dishes (2×10^5 cells/mL), and maintained in a tissue culture incubator overnight to allow adherent monolayer formation. After serum starvation, by culturing in a medium containing 3% FBS for 12 h, the cells were treated with different concentrations of STPE (0–1000 μg/mL) for 24 h. The culture medium was replaced with a thin layer of fresh Hank's Balanced Salt Solution (HBSS) (Hyclone, Logan, UT, USA) and cells were irradiated with the appropriate UVB dose using a UV spectral radiometer (VLX-3 W, Vilber Lourmat, France). HBSS was subsequently replaced with culture medium cotaining 3% FBS and incubated until analysis.

Cell viability assay

Cell viability was evaluated using 3-(4,5-dimethylthiazol-2-yl)-5-(3-carboxymethoxyphenyl)-2-(4-sulfophenyl)-2H-tetrazolium (MTS) using the CellTiter 96 Aqueous Non-Radioactive Cell Proliferation assay (Promega, Madison, WI, USA) according to the manufacturer's instructions. Briefly, L929 cells were seeded in 96-well plates at a density of 10^4 cells/well, and allowed to attach overnight. Cells were starved by culturing in a medium containing 3% FBS for 12 h. For the cytotoxicity profile evaluation, the cells were treated for 24 h with different concentrations of STPE. For the selection of the exposed dose, the cells were exposed to different doses of UVB (10, 20, 40, 80, 160, and 320 mJ/cm^2) and incubated for 24 h. For the protective evaluation under UVB rays, the cells were treated for 24 h with STPE, washed twice with HBSS, exposed to radiation, and incubated for a further 24 h. After the respective treatment conditions, 20 μL of MTS solution was added to wells for another 45 min, and the absorbance at 490 nm was measured with a microplate reader (Tecan, Männedorf, Switzerland). At least three independent experiments were performed.

ROS production

The intracellular accumulation of ROS was detected by 2,7-dichlorodihydrofluorescein diacetate (H_2DCF-DA) (D6883, Sigma-Aldrich, St. Louis, MO, USA). The cells were treated with STPE for 24 h and then incubated with 20 μM H_2DCF-DA for 30 min at 37 °C. Subsequently, the cells were washed three times with HBSS and exposed to 100 mJ/cm^2 UVB. Fluorescence was measured at 488/525 nm 1 h after UVB exposure using Tecan Infinite M200 PRO (Tecan).

Cellular antioxidant enzyme activity and lipid peroxidation

L929 cells were cultured in 60 mm tissue culture dishes at 1.6×10^6 cells/dish. After treatment with different

concentrations of STPE (0, 10, 20, and 40 μg/mL) for 24 h, the cells were exposed to 20 mJ/cm^2 UVB and incubated for a further 24 h. The cells were collected and resuspended in 400 μL of phosphate-buffered saline (PBS). The cells were disrupted using TissueLyser II (Qiagen, Hilden, Germany) and superoxide dismutase (SOD) and catalase (CAT) within the lysates were measured with appropriate assay kits (Jiancheng Bioengineering Institute, Nanjing, China) according to the manufacturer's instructions. Intracellular lipid peroxidation was evaluated by measuring malondialdehyde (MDA) production using a commercial kit (Jiancheng Bioengineering Institute, Nanjing, China).

RNA isolation, reverse transcription, and quantitative PCR (qPCR) analysis

The total RNA sample was collected and extracted using an RNAprep Pure kit (Tiangen Biotech, Beijing, China) 24 h after the end of UVB exposure at 10 mJ/cm^2. Reverse transcription was performed with 1 μg of total RNA using a PrimeScript RT Master Mix (Takara Bio, Otsu, Japan), and real-time qPCR was performed using a FastStart Universal SYBRGreen Master kit (Roche, Basel, Switzerland). The primers used for amplification of the target genes (inflammation-related genes, such as TNF-α, IL-1α, and IL-6) and the reference gene (succinate dehydrogenase complex flavoprotein subunit A, SDHA) are listed in Table 1. Relative quantification of target gene expression levels was performed using the $2^{-\Delta\Delta Ct}$ method.

Enzyme-linked immunosorbent assay (ELISA)

The cell culture supernatant was collected and concentrated 20 times in an ultrafilter tube prior to cytokine measurement by ELISA, according to the manufacturer's instructions. The ELISA kits for TNF-α, IL-6, and IL-1α were purchased from Novus Biologicals (Littleton, CO, USA) or ProteinTech (Wuhan, China). Absorbances were determined at 450 nm using a microplate spectrophotometer reader (Tecan), and the results are expressed as picograms (pg) of each cytokine/mL.

Western blotting

For NF-κB nuclear translocation analysis, after 24 h of UVB irradiation, the separation of cytosolic and nuclear components of L929 cells was performed using NE-PER nuclear and cytoplasmic extraction reagents (Thermo Fisher Scientific), according to the manufacturer's instructions. The amount of protein was estimated using the PierceTM BCA Protein Assay Kit (Thermo Fisher Scientific). Afterward, equal amounts of protein were collected and heated at 100 °C for 5 min in a loading buffer. The proteins were electrophoresed on a 12% SDS-polyacrylamide gel and transferred to a polyvinylidene fluoride membrane (Pall Corporation, NY, USA) in a transfer buffer (25 mM Tris base, 250 mM glycine, 20% methanol). The membranes were blocked with 5% skim milk (BD Difco, NJ, USA) in PBS containing 0.05% Tween 20 buffer overnight at 4 °C and incubated with primary antibodies (NF-κB p65 (D14E12) XP Rabbit mAb, p-NF-κB p65 (Ser536) (93H1) rabbit mAb, anti-IκBα antibody, anti-SDHA antibody, and anti-Lamin B antibody) for 2 h at room temperature. Membranes were washed and incubated with horseradish peroxidase-conjugated goat anti-rabbit IgG secondary antibody for 1 h at room temperature. The antigen-antibody complex was detected by chemiluminescence using ECL detection reagent (Advansta, CA, USA) and analyzed using the ChemiDoc® XRS+ Imaging System (Tanon-5200 s, Tanon, Shanghai, China) (Additional file 1).

Hoechst 33342 staining

The intensity of nuclear condensation was examined using the cell-permeable DNA dye Hoechst 33342. The probe (2 μg/mL) was added after 24 h of UVB exposure, and cells were incubated for 20 min at 37 °C and washed twice with PBS. The cells were then visualized

Table 1 Primers used for real-time qPCR

Gene	Primer sequence (5′ → 3′)	GenBank accession No.	Reference
SDHA	GGAACACTCCAAAAACAGACCT CCACCACTGGGTATTGAGTAGAA	NM_023281	–
IL-1α	TCTATGATGCAAGCTATGGCTCA CGGCTCTCCTTGAAGGTGA	NM_010554	–
IL-6	CCCAATTTCCAATGCTCTCC TCCACAAACTGATATGCTTAGG	NM_031168	[16]
TNF-α	ACAAGGCTGCCCCGACTAC TGGAAGACTCCTCCCAGGTATATG	NM_013693	

under a fluorescence microscope (DMI8, Leica, Wetzlar, German).

Effects of STPE on zebrafish growth

Embryos of AB wild-type zebrafish developed at 2 days post-fertilization (dpf) were collected and randomly divided into 30 embryos per experimental group. Embryos were treated with STPE at concentrations of 5, 10, 25, 100, 250, 500, 1000, and 2000 μg/mL for 24 h, and exposed to UVB generated by an ultraviolet light therapy instrument (KN-4006, Kernel Medical Equipment, Xuzhou, China) at 3 dpf. For UVB exposure, each group was exposed five times separated by 30 min intervals. Each exposure delivered 8100 mJ/cm^2 (9 mW/cm^2, 15 min) of energy. After UVB exposure, all embryos were cultivated in 6-well cell culture plates and the survival rates were counted at 5 dpf. The study was carried out in compliance with the ARRIVE (Animal Research: Reporting of In Vivo Experiments) guidelines.

Repairing effect of STPE on caudal fin damage in UVB-irradiated zebrafish

Embryos developed at 2 dpf were collected and randomly divided into 30 embryos per experimental group. Embryos were treated with different concentrations of STPE (0.56, 1.67, and 5 μg/mL) or epigallocatechin gallate (EGCG; 30 μg/mL) for 24 h. After UVB exposure at 3 dpf, all embryos were cultivated in 6-well cell culture plates at 28 °C until 5 dpf. The culture medium was changed daily throughout the experiment. Ten zebrafish were randomly selected from each group to observe their tails under a dissecting microscope (SZX7, Olympus, Tokyo, Japan). Images were taken and analyzed using an image processing software (NIS-Elements D 4.30.00) to calculate the area of the caudal fin of the larva. The caudal fin area was used to evaluate the effect of STPE on the repair of UV irradiation-induced skin damage in zebrafish. Skin damage repair of zebrafish was calculated using the following formula: Repairing effect (%) $= \frac{S_{STPE}-S_{UVB}}{S_{UVB}} \times 100\%$. The study was carried out in compliance with the ARRIVE guidelines.

Effect of STPE on ROS scavenging in UVB-irradiated zebrafish

Embryos developed at 2 dpf were collected and randomly divided into 30 embryos per experimental group. Embryos were treated with different concentrations of STPE (0.8, 1.2, and 1.6 μg/mL) or EGCG (30 μg/mL) for 24 h. After 2 h of UVB exposure at 3 dpf, embryos were incubated with 500 ng/mL CM-H_2DCF-DA (Invitrogen, Waltham, USA) for 20 h. The embryos were subsequently placed in a 96-well blackboard (1 per well, 8 per group). The fluorescence intensity of the embryo (FI) was measured at excitation/emission = 485/535 nm (Tecan, Austria). The effect of STPE on oxygen radical scavenging in zebrafish was calculated as follows: $\text{ROS scavenging rate } (\%) = \frac{(FI_{UVB}-FI_{Blank})-(FI_{STPE+UVB}-FI_{Blank})}{FI_{UVB}-FI_{Blank}} \times 100\%$. The study was carried out in compliance with the ARRIVE guidelines.

HPLC-MS/MS analyses

STPE was analyzed on a Thermo Ultimate 3000 LC system coupled with a Thermo Q Exactive HF system (Thermo Fisher Scientific, Waltham, USA). Chromatographic analyses were carried out on Zorbax Eclipse C18 (2.1 × 100 mm,1.8 μm, Agilent Technologies). The mobile phase consisted of two solvents: 0.1% formic acid in water (A) and acetonitrile (B). Elution was performed with linear gradient elution as follows: 0–2 min, 5% B; 2–6 min, 5–30% B; 6–7 min, 30% B; 7–12 min, 30–78% B; 12–14 min, 78% B; 14–17 min, 78–95% B; 17–20 min, 95% B; 20–21 min, 95–5% B; 21–25 min, 5% B. The flow rate was 0.3 mL/min and the injection volume was 2 μL.

The mass spectrometer was operated in both positive and negative ion modes and full MS (m/z 100–1500)/data-dependent MS^2 (dd-MS^2, TopN = 10) mode. The mass parameters were as follows: spray voltage 3.5 kV; capillary temperature 330 °C; sheath gas (N_2) flow rate 45 arb; auxiliary gas (N_2) flow rate 15 arb; probe heater temperature 325 °C; and S-Lens RF level 55%. Retention time correction, peak identification, peak extraction, etc. were performed using Compound Discoverer 3.2. The identification of individual phenolic compounds was based on their retention time, mass spectrometry, and their mass-to-charge (m/z) ratio as compared with local brown algae polyphenol database constructed based on previous literature.

Results

STPE reverses the UVB-induced decrease in cell viability

S. thunbergii was extracted twice at 70 °C with 40% anhydrous ethanol, and then purified with the macroporous adsorbent resin XDA-7 to obtain STPE. The total polyphenol content of STPE was 72% as determined using the colorimetric Folin–Ciocalteu method.

To determine STPE cytotoxicity, L929 cells were treated with various concentrations of STPE (0–320 μg/mL) for 24 h. STPE at concentrations of 10–40 μg/mL had no effect on cell viability compared to the untreated group ($p > 0.05$; Fig. 1a), although cytotoxicity was observed at 80 μg/mL ($p < 0.05$). Based on this, 10–40 μg/mL STPE was used in subsequent assays. Cells were treated with various doses of UVB (0–320 mJ/cm^2) and cultured for 24 h to determine the appropriate irradiation dose to induce photodamage. UVB reduced cell viability in a concentration-dependent manner (Fig. 1b); 20 mJ/cm^2 UVB decreased cell

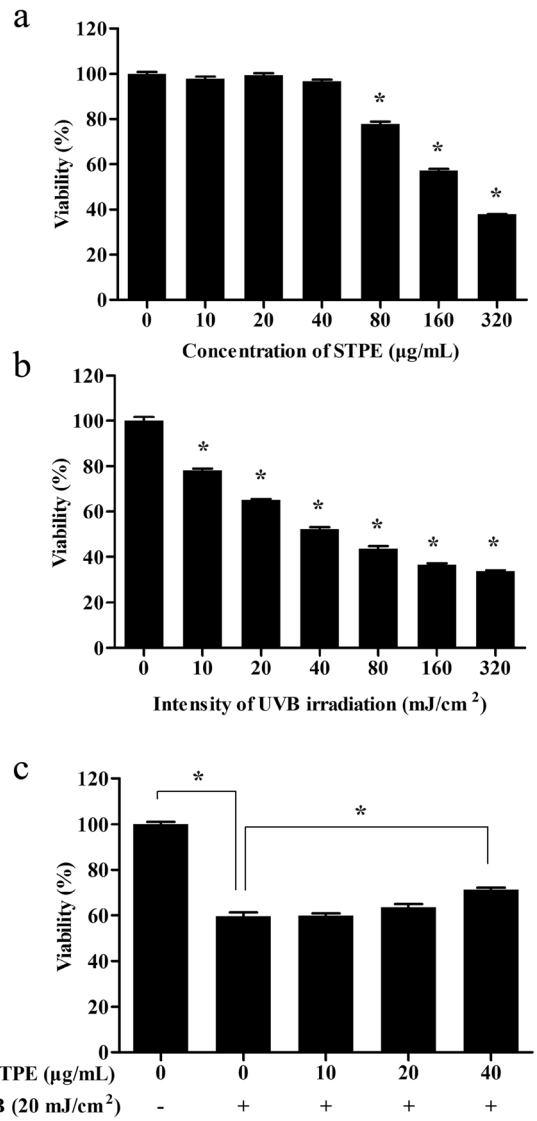

Fig. 1 STPE reverses the UVB-induced decrease in cell viability. The effects of (**a**) STPE and (**b**) UVB at different concentrations or dose on L929 cell viability, and (**c**) the protective effects of STPE on L929 cell damage by UVB (20 mJ/cm^2). The error bars refer to the standard deviations obtained from six sample analyses. The data were analyzed by one-way ANOVA followed by LSD post-hoc test. Means with "*" differ significantly ($p < 0.05$)

viability by approximately 50% and was selected as the UVB dose in subsequent experiments. Cell viability was reduced to 60% following exposure to UVB alone compared with that of the experimental control (Fig. 1c). However, pretreatment of cells with STPE (10–40 μg/mL) reversed this effect in a concentration-dependent manner, and was significantly different at 40 μg/mL from that of the UVB model group.

STPE inhibits oxidative stress and lipid peroxidation

The intracellular ROS scavenging effects of STPE induced by UVB were assessed using H_2DCF-DA oxidant-sensitive fluorescent probes. The scavenging effect of STPE on the intracellular ROS generated by UVB exposure was measured using a microplate reader (Fig. 2a). The ROS level in UVB-exposed cells increased 2.35-fold compared with that in control cells. However, 24 h pretreatment of cells with increasing concentrations of STPE resulted in a concentration-dependent reduction of intracellular ROS.

SOD and CAT are important antioxidant enzymes that protect tissues from oxidative damage. MDA production is used to evaluate intracellular lipid peroxidation owing to oxidative stress. The protective mechanisms of STPE were evaluated by measuring the levels of SOD, CAT, and MDA. Compared with those in the control group, SOD levels decreased following UVB exposure; however, this was abrogated by STPE pretreatment at 20 and 40 μg/mL (Fig. 2c). CAT activity was elevated after STPE treatment at 40 μg/mL (Fig. 2d). The increase in MDA content (Fig. 2b) induced by UVB ($p < 0.05$) was reversed by pretreatment with 40 μg/mL STPE ($p < 0.05$).

STPE alleviates UVB-induced inflammation in L929 cells

To evaluate the effects of STPE on inflammatory cytokine production in UVB-exposed L929 cells, the mRNA and protein expression levels were measured by real-time qPCR (Fig. 3a) and ELISA (Fig. 3b), respectively. UVB exposure stimulated the expression of *TNF-α*, *IL-1α*, and *IL-6* mRNA compared with control cells. However, treatment with 40 μg/mL STPE decreased *TNF-α* and *IL-6* mRNA expression levels. STPE reduced UVB-induced TNF-α, IL-6, and IL-1α protein production in a dose-dependent manner.

STPE inhibits NF-κB activation in UVB-induced L929 cells

NF-κB plays an important role in immune responses, and dysregulation of NF-κB is associated with various diseases such as cancer, inflammation, and aging [17]. UVB increased both the protein levels of NF-κB p65 and p-p65 (Ser536) in the nucleus, whereas treatment with STPE decreased the nuclear p-p65 (Ser536) protein levels in a dose-dependent manner (Fig. 4). The protein expression levels of p65 did not decrease in the nucleus after STPE incubation. Additionally, STPE pretreatment significantly increased NF-κB (p65) expression in the cytoplasm. IκBs are upstream regulators of the NF-κB signaling pathway. In cells that are not stimulated, NF-κB dimers are present in an inactive state by binding to IκBs. IκBs are degraded by ubiquitination; thus, NF-κB

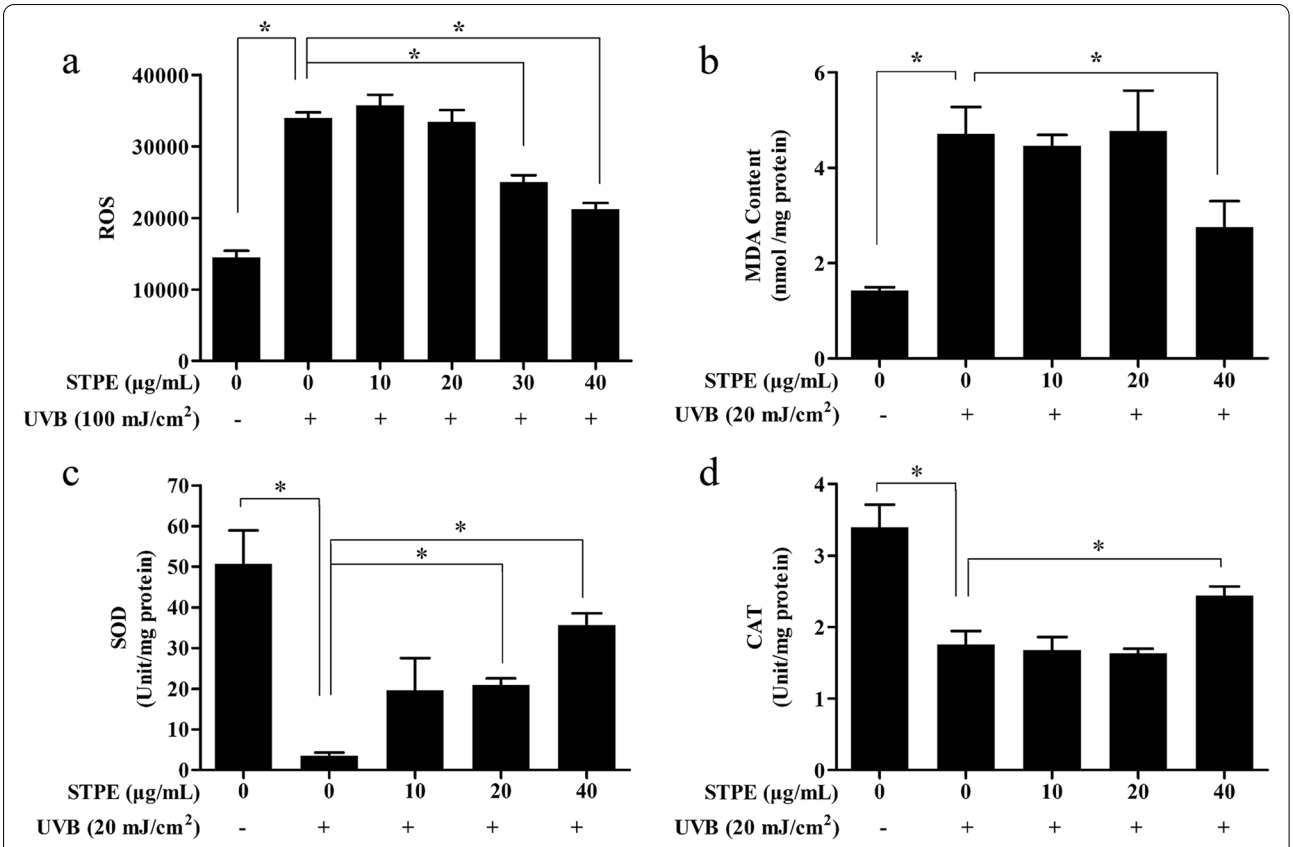

Fig. 2 STPE inhibits UVB-induced oxidative stress and lipid peroxidation. Effects of STPE on (**a**) ROS and (**b**) MDA content as well as (**c**) SOD and (**d**) CAT activities in L929 cells. Means with "*" differ significantly ($p < 0.05$)

is translocated from the cytoplasm to the nucleus, causing an inflammatory response following UVB exposure [18]. Our results showed that treatment with STPE at 40 μg/mL significantly enhanced IκBα expression. The increased protein levels of cytoplasmic NF-κB (p65) and IκBα indicated that STPE prevents NF-κB from entering the nucleus.

STPE attenuates DNA condensation in UVB-treated L929 cells

To evaluate nuclear alterations, DNA condensation was analyzed and visualized by fluorescence microscopy (Fig. 5). The fluorescent probe, Hoechst, was used to evaluate DNA condensation. Cells with homogeneously stained nuclei were considered viable, whereas cells stained strongly with an intense blue color were indicative of apoptosis [19]. Untreated cells displayed intact nuclei, whereas UVB-irradiated cells exhibited significant nuclear condensation (bright blue staining), suggesting these cells were undergoing the apoptotic process. Pretreatment with 20 and 40 μg/mL STPE significantly reversed DNA condensation compared with the UVB control.

Repairing effect of STPE on caudal fin damage in UVB-irradiated zebrafish

Zebrafish have been widely used in recent years as an in vivo oxidative stress model to study the protective effects of UV radiation. Schematic representation of the experimental protocols was shown in Fig. 6a. This study first explored the effects of STPE on the growth of wild-type AB strain zebrafish, thereby providing data on the maximum safe STPE concentration for subsequent experiments (Additional file 1). STPE induced high mortality at concentrations of 10 μg/mL and above after UV irradiation. No significant abnormalities were observed at 5 μg/mL STPE; therefore, this was the maximum experimental concentration used in the zebrafish UV damage model.

The potential of STPE to repair skin damage in zebrafish exposed to UVB radiation is shown in Fig. 6b and c. Using a deconvolution microscope, the caudal fin of zebrafish displayed a rough and crinkled phenotype after exposure to UV radiation. Treatment of zebrafish with 30 μg/mL of EGCG showed 182,115 ± 8402 pixels in the tail fin area of zebrafish, compared to only 141,544 ± 5864 pixels in the tail fin area of the

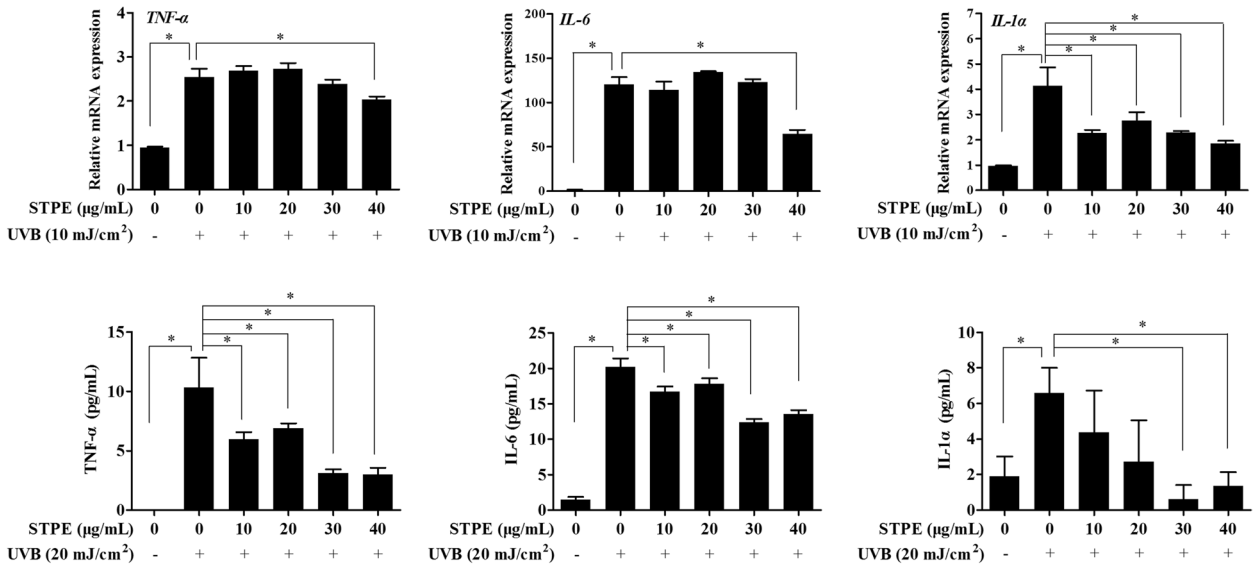

Fig. 3 STPE inhibits UVB-induced pro-inflammatory cytokine mRNA expression and secreted production in L929 cells. Cells were pretreated with different concentrations of STPE (0, 10, 20, and 40 μg/mL) for 24 h. **a** The mRNA expression of TNF-α, IL-6, and IL-1α in L929 cells was measured by qPCR at 24 h after the end of exposure to 10 mJ/cm^2 UVB. **b** Cell culture supernatants were collected to measure cytokine production at 24 h after the UVB exposure (20 mJ/cm^2). Bars represent means ± SEM of four samples per group. The data were analyzed by one-way ANOVA followed by LSD post-hoc test. Means with "*" differ significantly ($p < 0.05$)

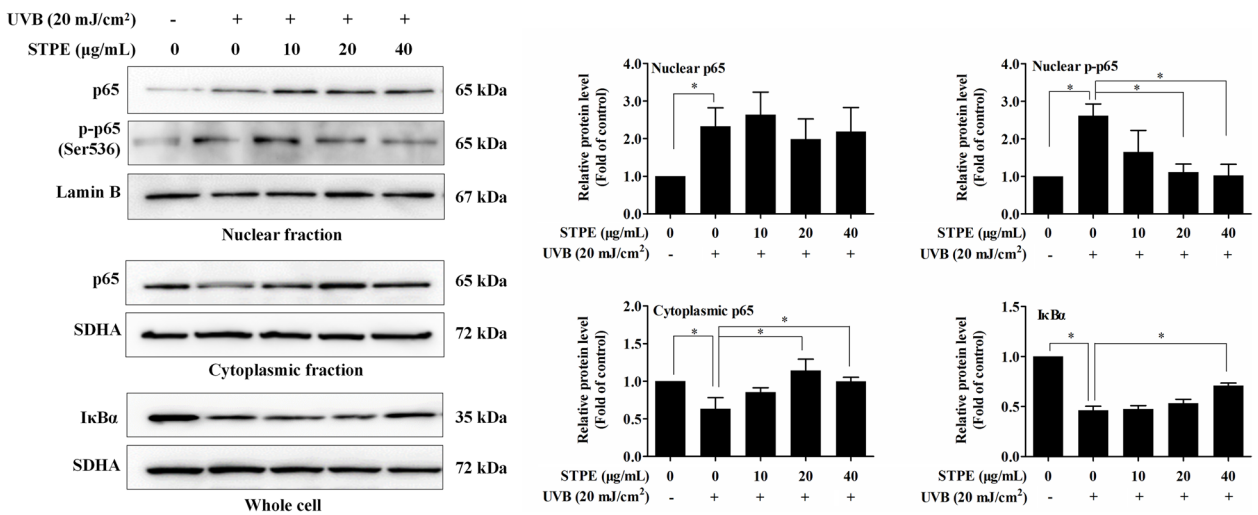

Fig. 4 Effects of STPE on NF-κB translocation and I-κB***α*** expression in UVB-induced L929 cells. Western blot analysis showing the effect of STPE treatment on the expression of p65 and p-p65 in nuclear extracts, p65 in cytoplasmic extract, and I-κB***α*** in the whole cell. Cytosolic proteins were normalized with SDHA and nuclear proteins were normalized with laminin B. The cells were grown in 6-well cell culture plates and treated with various concentrations of STPE for 24 h before UVB (20 mJ/cm^2) treatment. After incubation for 24 h, cell lysates were collected and subjected to western blot analysis using antibodies specific for p65, p-p65, and I-κB***α***. Intensity quantification of protein bands were analyzed by Quantity One software (Bio-Rad). Bars represent means ± SEM of three samples per group. The data were analyzed by one-way ANOVA followed by LSD post-hoc test. Means with "*" differ significantly ($p < 0.05$)

control zebrafish model. The effect of tea polyphenols on the repair of zebrafish skin damage was 29%, indicating that the positive control treatment significantly repaired zebrafish skin damage. Treatment of zebrafish with 0.56, 1.67, and 5 μg/mL of STPE resulted in a caudal fin area of 145,518 ± 4608 ($p > 0.05$), 174,965 ± 3632

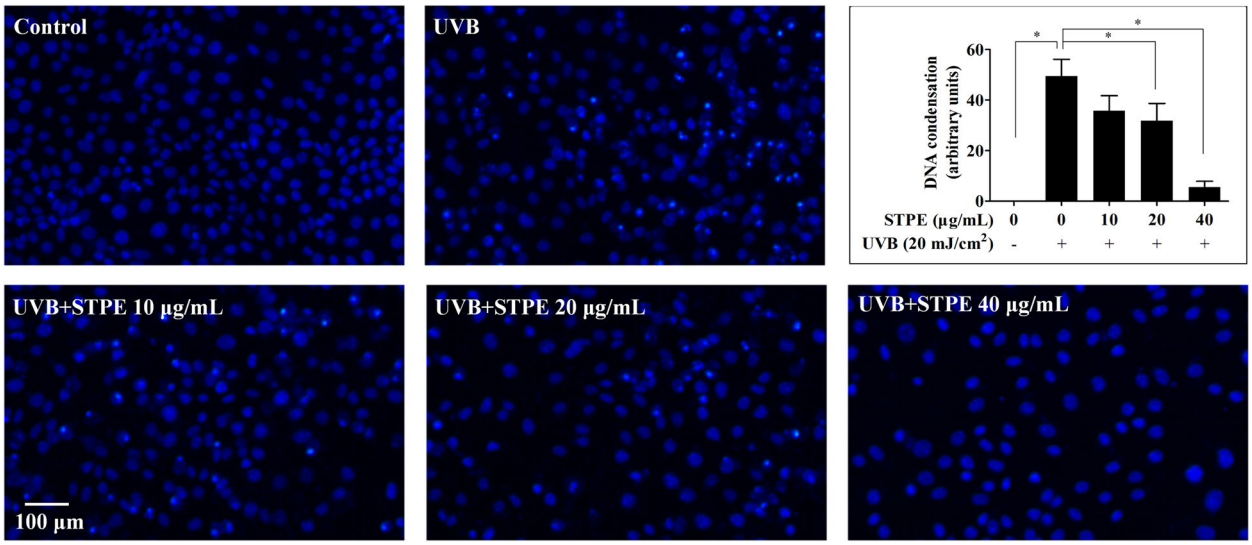

Fig. 5 Evaluation of DNA protection in UVB-irradiated L929 fibroblasts pretreated with STPE. Apoptotic body formation was observed under a fluorescence microscope following Hoechst 33342 staining. Bars represent means ± SEM of four samples per group. The data were analyzed by one-way ANOVA followed by LSD post-hoc test. Means with "*" differ significantly ($p < 0.05$)

($p < 0.001$), and 149,357 ± 5283 ($p > 0.05$) pixels, respectively, compared with that of the control model; the effects on skin damage repair were 3, 24, and 6%, respectively. Collectively, STPE showed a significant restorative effect on zebrafish skin damage.

ROS scavenging effect of STPE on UVB-radiated zebrafish

The effects of STPE on UVB-mediated ROS induction in zebrafish are shown in Fig. 6d. The fluorescence value of the UVB group was 6271 ± 264 ($p < 0.001$), which was higher than that of the normal controls (1169 ± 124), indicating successful model establishment. The fluorescence values of the 30 μg/mL EGCG-positive control group (1122 ± 39) were reduced by 82% ($p < 0.001$) compared with those of the UVB group. The fluorescence values of the STPE group at 0.8, 1.2, and 1.6 μg/mL concentrations were 1818 ± 78, 1834 ± 116, and 950 ± 30, respectively, at which the intracellular ROS accumulation decreased by 71, 71, and 85% ($p < 0.001$), respectively, compared with those of the UVB group. These findings demonstrated that STPE had a significant scavenging effect on ROS in this zebrafish model.

Phenolic profile of STPE

The total ion chromatogram for the determination of STPE in negative ion mode is shown in Fig. 7a. To extract information about the phenolic compounds, the names and molecular formulae of 144 phenolic compounds were collected from professional databases (Pubchem, ChemSpider, Scifinder and Huaxuejia) and references related to the phenolic extracts of brown algae, and their exact relative molecular masses were calculated. 14 phenolic compounds identified from STPE, which included 4 Benzene and substituted derivatives, 1 Cinnamic acids and derivatives, 4 Flavonoids and 5 phlorotannins (Table 2). The extracted ion chromatograms are shown in Fig. 7b.

Discussion

UVB radiation causes a series of adverse skin reactions, such as erythema, sunburn, photoaging, and cancer, by altering the signaling pathways related to inflammation and oxidative stress. Therefore, improving UVB-induced inflammation and oxidative stress is a potential tool for preventing and protecting against UVB-induced cellular and tissue photodamage [20]. In this regard, several edible and medicinal plants have been used to mitigate UVB-exposed skin damage. The present study demonstrates the inhibitory effect of *S. thunbergii* against UVB-induced oxidative stress and inflammation, suggesting the potential photoprotective effect of STPE in UVB-irradiated L929 cells in vitro, as well as zebrafish in vivo.

L929, a mouse fibroblast cell line, has been used for phototoxicity assessment, and the results were compared with the OECD-approved NIH-3 T3 cell line [12]. The study showed that the L929 cell line, with UVR, was found to be an equally potential in vitro screening test system for the photosensitivity evaluation of drugs/chemicals; thus, it could be used as an in vitro screening test system for phototoxicity assessment. At the same time, the literature also shows that many studies have

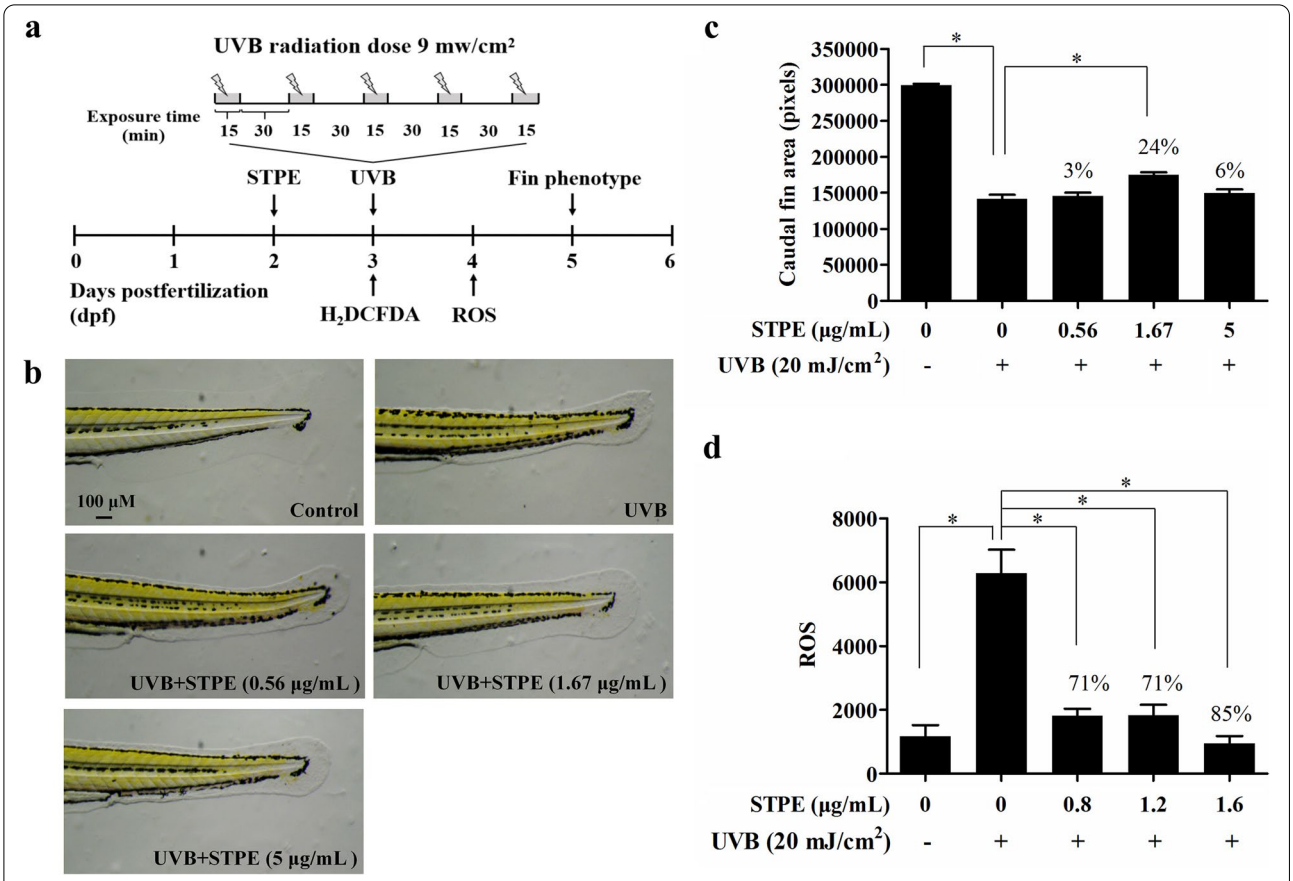

Fig. 6 Evaluation of photoprotective effect of STPE on UVB-irradiated zebrafish. Zebrafish embryos at 2 days post-fertilization (dpf) were used. **a** Schematic representation of the experimental protocols performed in this study. **b**, **c** UVB-induced malformed fin phenotypes can be attenuated by STPE. **d** Inhibitory effect of STPE on UVB-induced ROS generation in zebrafish. Results were analyzed using one-way ANOVA with post-hoc Dunnett's t-test. Differences with a *p* value of less than 0.05 were considered statistically significant and denoted by "*"

used L929 fibroblast cell lines as a target of UVB-induced photoaging and photodamage [21–24], which also suggested the suitability of mouse L929 as an in vitro model of photodamage.

UVB induces ROS generation via the BLT2-Nox1-linked pathways, and leads to the depletion of antioxidant defenses either by exhausting their activity or directly damaging proteins [4, 25]. Excessive ROS attack the cell membrane and cellular organelles, resulting in lipid peroxidation and organelle damage, which further induce inflammation and apoptosis in human skin cells [26]. To reduce the negative impact of UV radiation, many marine organisms that photosynthesize have adapted to evolve multiple photoprotective mechanisms against UV radiation [27]. Under UVB radiation, plants alter their phenolic metabolism and provide phenolic compounds to shield against the UVB rays, and act as an antioxidant to decrease UVB-mediated ROS production [28]. In our study, STPE possessed ROS clearance in both L929 cells and zebrafish models. The ROS scavenging ability of brown algae polyphenol in relation to skin protection against UVB have been widely demonstrated. Heo et al. [29] demonstrated for the first time that dieckol extracted from *E. cava* possesses potential inhibitory effects on intracellular oxidative damage induced by UVB radiation. Ko et al. [30] compared the protective effects of extracts from six species of brown seaweed. The results indicated that dieckol from *E. cava* exhibits a higher protective effect against UVB-induced cell damage in HaCaT cells. Moreover, ROS, nitric oxide, and cell death levels in live zebrafish induced by UVB radiation are reduced following the addition of dieckol.

Previous studies have shown that the expression of several enzymes (CAT, SOD, glutathione transferase, nicotinamide adenine dinucleotide (phosphate) quinone oxidoreductase, and hemoxygenase-1) in skin is affected following exposure to UVB radiation [31]. MDA is a marker of lipid peroxidation and cell injury. Thus, we sought to measure the SOD, CAT, and MDA levels in L929 cells to evaluate the antioxidative effects of STPE.

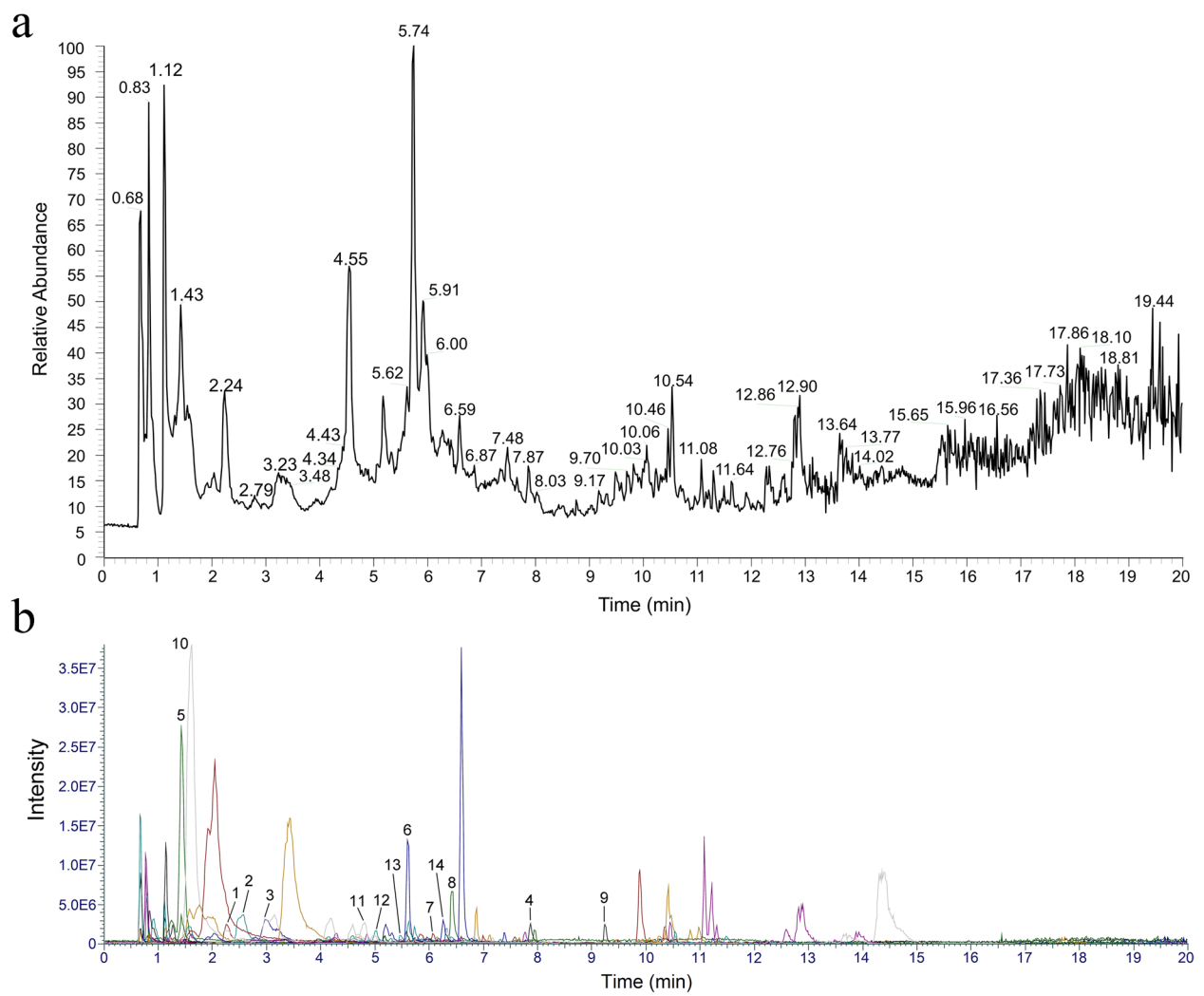

Fig. 7 Total ion chromatogram (**a**) and Overlaid extracted ion chromatogram (EIC) acquired in negative ion mode (**b**) for STPE. Peaks refer to Table 2

The result showed that STPE enhanced SOD and CAT activity and suppressed MDA production in UVB-irradiated L929 cells. This result was similar with that reported by Jang et al. [32], who reported that phlorotannins eckstolonol from *E. cava* reduced photo-oxidative stress and DNA damage by scavenging ROS and enhancing CAT and SOD activities. The ethyl acetate fraction of *Sargassum muticum* increased the protein expression levels of both Cu/Zn SOD and CAT in a time-dependent manner compared with that of UVB-exposed HaCaT cells [33]. Quercitrin, which also isolated from many brown algae, restored CAT expression and GSH/GSSG ratio reduced by UVB exposure, leading to reductions of oxidative DNA damage and apoptosis and protection of the skin from inflammation caused by UVB exposure [34].

With respect to the mechanism of antioxidant enzyme activity restoration, it has been demonstrated that natural sourced antioxidants regulate the signaling pathways related to the expression of antioxidant enzymes, such as Nrf2-Keap1-ARE, NF-κB and MAPK [35]. Nrf2 regulates the antioxidant factors, including quinone oxidoreductase 1, heme Oxygenase-1, SOD and CAT [36]. During activation of the NF-κB pathway, intranuclear p65 negatively regulates the Nrf2 pathway by competing with the transcriptional co-activator CREB-binding protein (CBP)-p300 complex limiting the availability of CBP for Nrf2 complex formation [37]. In our study treatment with STPE significantly decreased the nuclear p-p65 (Ser536) protein levels, which might release more CBP to bind to Nrf2, subsequently restoring the activities of antioxidant enzymes, such as SOD and CAT. Similar results was found with tea polyphenol pretreatment which significantly inhibited the activation of NF-κB and promoted the activities of SOD, CAT, and GSH-Px [38].

Table 2 Peak assignments of brown algae phenolic compounds detected in STPE

No.	RT (min)	Compond	Formula	Class	$[M-H]^-$ m/z
1	2.27	protocatechuic acid	$C_7H_6O_4$	Benzene and substituted derivatives	153.01883
2	2.55	difucol	$C_{12}H_{10}O_6$	Benzene and substituted derivatives	249.04079
3	2.99	gallic acid	$C_7H_6O_5$	Benzene and substituted derivatives	169.01376
4	7.87	4-hydroxybenzoic	$C_7H_6O_3$	Benzene and substituted derivatives	137.02383
5	1.43	p-Coumaric acid	$C_9H_8O_3$	Cinnamic acids and derivatives	163.0396
6	5.60	Isoquercitrin	$C_{21}H_{20}O_{12}$	Flavonoids	463.08957
7	6.07	quercitrin	$C_{21}H_{20}O_{11}$	Flavonoids	447.09467
8	6.42	isorhamnetin	$C_{16}H_{12}O_7$	Flavonoids	315.05206
9	9.24	catechin	$C_{15}H_{14}O_6$	Flavonoids	289.07248
10	1.62	bifuhalol	$C_{12}H_{10}O_7$	Tannins	265.03595
11	4.81	pentafuhalol A	$C_{30}H_{22}O_{17}$	Tannins	653.08099
12	5.01	7-hydroxyeckol	$C_{18}H_{12}O_{10}$	Tannins	387.03696
13	5.48	deshydroxypentafuhalol	$C_{30}H_{22}O_{16}$	Tannins	637.08289
14	6.33	trifuhalolA	$C_{18}H_{14}O_{10}$	Tannins	389.05243

Most UVB-associated diseases share inflammation-related characteristics, such as upregulated pro-inflammatory cytokine levels and the activation of transcription factors, including NF-κB [39, 40]. This, in turn, propagates inflammation-induced signals and aggravates skin aging or disease by inducing apoptosis and increasing ROS production [41]. Martinez et al. [4] reported that UVB irradiation increases the production of several pro-inflammatory cytokines, including TNF-α, IL-1β, and IL-6, as well as Th1, Th2, and Th17 cytokines, and anti-inflammatory cytokines (IL-10 and TGF-β) in the skin of hairless mice. Findings from our study confirmed that UVB markedly induced the gene and protein expression of TNF-α, IL-6, and IL-1α in L929 cells, which was effectively suppressed by pretreatment with STPE. Phenolic compounds have been shown to be potentially useful to treat many inflammatory diseases. Brown algae polyphenol treatment inhibits the expression levels of inflammatory mediators (nitric oxide, iNOS, and COX-2) at the transcriptional level in a *Propionibacterium acnes*-induced HaCaT cell model [42] and macrophage-derived chemokine MDC/CCL22 production in an IFN-γ-induced skin inflammation model [43]. The expression of iNOS, COX-2, TNF-α, IL-6, and HMGB-1 is inhibited following phlorotannin treatment in a lipopolysaccharide-induced sepsis model [44]. NF-κB activation has been shown to regulate the production of a variety of pro-inflammatory cytokines. NF-κB is composed of p65 and p50 subunits and is sequestered in the cytoplasm by its inhibitory proteins, I-κBs. NF-κB p65 can be activated and rapidly transported from the cytoplasm to the nucleus during the phosphorylation and degradation of I-κBs. Herein, STPE inhibited the activation of NF-κB in UVB-irradiated L929 cells, which was supported by a decrease in the phosphorylation of the p65 subunit in the nucleus. Moreover, NF-κB (p65) expression in the cytoplasm and IκB expression were significantly increased by STPE, which also indicated the inhibition of NF-κB activation. Our data suggested that STPE inhibits the UVB-induced inflammatory process in L929 cells through the NF-κB signaling pathway. These results are corroborated by previous reports showing that the purified phlorotannins fucofuroeckol-A and 8,8′-bieckol can reduce the production of pro-inflammatory cytokines via the suppression of NF-κB signaling [45, 46]. Diphlorethohydroxycarmalol (DPHC), isolated from the brown algae *I. okamurae*, suppresses intracellular ROS, collagenase, and elastase production and reduces the expression of MMPs and pro-inflammatory cytokines by regulating the NF-κB, AP-1, and MAPKs signaling pathways in UVB-irradiated human dermal fibroblasts [47].

The zebrafish, a small tropical freshwater fish, has become a useful vertebrate model organism owing to its small size, large clutches, transparency, low cost, and physiological similarity to mammals [48]. Previous studies have used zebrafish as a system for evaluating the efficacy of other UVB protective compounds by assessing fin damage and measuring ROS generation [13, 14]. Our results demonstrated that zebrafish fins in the UVB and STPE combined groups were more likely to phenotypically return to normal than fins in the UVB only-treated group. Additionally, STPE significantly reduced ROS production in the UV-exposed zebrafish embryos. The protective effect of phlorotannin extracts on UVB-radiated

zebrafish has been previously reported. For example, DPHC isolated from *I. okamurae* confers in vivo protection against photodamage by decreasing cell death, as well as reducing lipid peroxidation and inflammatory responses by decreasing ROS levels in UVB-irradiated zebrafish [47]. The ethyl acetate fraction of 70% ethanol extracts of *Spirogyra* sp. reduces ROS generation in UVB-irradiated zebrafish [49]. Additionally, Guinea et al. [50] showed that the phenolic extracts from *Macrocystis pyrifera* and *Porphyra columbina* exhibit good photoprotective activity in zebrafish embryo models.

Acute and chronic exposure of skin cells to UVB can cause apoptosis [25], characterized by membrane blebbing and nuclear fragmentation. Skin cells exposed to UVB irradiation may respond by activating protective mechanisms or eventually undergo apoptosis [51]. To further study the protective effect of STPE against UVB radiation-induced apoptosis in L929 cells, apoptotic body formation was observed following Hoechst 33342 staining. Our results showed that UVB greatly enhanced DNA condensation; however, this was significantly decreased by STPE pretreatment. The inhibition of apoptosis by brown algae polyphenol has been previously reported. For example, the suppressive effect of fucodiphlorethol G on apoptotic body formation by UVB radiation has been observed using Hoechst 33342 staining methods [8]. Dioxinodehydroeckol, a phlorotannin from *E. cava*, prevents UVB-induced apoptosis in HaCaT cells [52]. Eckol and triphlorethol-A compounds, purified from *E. cava,* exhibit protective effects against UVB radiation-induced cell damage and apoptosis in human keratinocytes [53, 54].

We identified 14 phenolic compounds from STPE, some of which have been reported to protect skin or skin cells from UVB damage. For example, p-coumaric acid has been reported to attenuate UVB-induced release of stratifin from HaCaT cells and indirectly regulate matrix metalloproteinase 1 release from fibroblasts [55]. Isoquercitrin exhibited antioxidant activity and UVB-induced generation of photoaging-related factor inhibition without showing any toxicity [56]. Gallic acid regulates skin photoaging in both fibroblast and mice model [57]. Quercitrin decreased ROS generation and restored the levels of two major antioxidant enzymes, leading to reductions

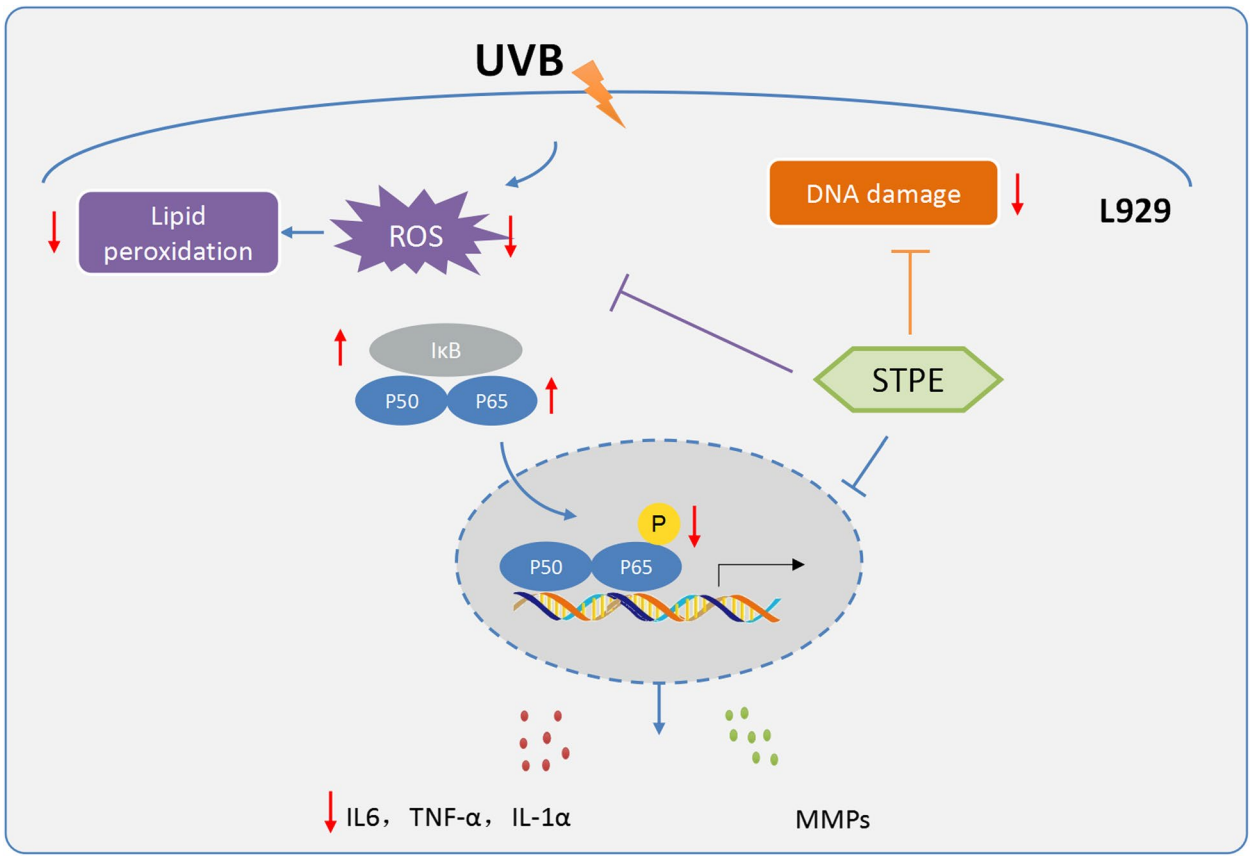

Fig. 8 Schematic diagram showing the effects of STPE on UVB induced photodamage

in UVB-induced oxidative damage [34]. Based on previous reports, the photoprotective activity of STPE may be the result of the combined effect of multiple phenolic compounds.

Conclusions

In the present study, we isolated phenolic-rich extract from *S. thunbergii*, and evaluated its protective effects against UVB-induced photodamage, both in vitro using L929 cells and in vivo using zebrafish models. Our data suggest that the protective effects against UVB are mediated through the antioxidant, anti-inflammatory, and anti-apoptotic capacity of STPE by regulating NF-κB signaling pathways (Fig. 8). This study helps to expand our understanding of the protective activity of STPE on skin. However, the pure phenolic compound of STPE with photoprotective activity was not obtained. We will continue to work on obtaining a highly purified and stable STPE molecule for further application as a potential protective agent to prevent skin damage caused by UVB in pharmaceutical and cosmeceutical industries.

Abbreviations

CAT: Catalase; dpf: Days post-fertilization; EGCG: Epigallocatechin gallate; ELISA: Enzyme-linked immunosorbent assay; FBS: Fetal bovine serum; FI: Fluorescence intensity of the embryo; HBSS: Hank's Balanced Salt Solution; H_2DCF-DA: 2,7-dichlorodihydrofluorescein diacetate; MDA: Malondialdehyde; MTS: 3-(4,5-dimethylthiazol-2-yl)-5-(3-carboxymethoxyphenyl)-2-(4-sulfophenyl)-2H-tetrazolium; NF-κB: Nuclear Factor KappaB; PBS: Phosphate-buffered saline; qPCR: Quantitative PCR; ROS: Reactive oxygen species; SDHA: Succinate dehydrogenase complex flavoprotein subunit A; SOD: Superoxide dismutase; STPE: *S. thunbergii* phenolic-rich extract; UV: Ultraviolet; UVB: Ultraviolet B.

Supplementary Information

The online version contains supplementary material available at https://doi.org/10.1186/s12906-022-03609-x.

Additional file 1.

Acknowledgments

We extend our special thanks to Peng Zhang (Mariculture Research Institute of Zhejiang, China) and Chenhui Zhong (Fisheries Research Institute of Fujian Province, China) for providing us with the algae of *S. thunbergii* and Yutian Pan (the Engineering Technological Center of Mushroom Industry, Minnan Normal University, China) for providing us with the L929 cell line. We would like to thank Hunter Biotechnology, Inc. for proceeding zebrafish experiment and Editage (www.editage.cn) for English language editing.

Authors' contributions

BC, HDQ and KQ carried out the UVB exposed experiment and drafted the manuscript. HHC and YCS performed collection and extraction of brown algae, and isolation of compound. MX and JNW carried out the antioxidant assay and contributed to data analysis. YS helped to designed the zebrafish experiment. ZYL and QW designed the experiment, participated in general coordination of the study and provided critical revision of the manuscript. All authors read and approved the final manuscript.

Funding

This work was supported by the Province-owned Public Scientific Research Institutes in Fujian Province (2017R1003–13) and Xiamen Special Fund Project for Marine Economic Development (21CZP002HJ05).

Availability of data and materials

The gene analyzed during the current study are available from Genbank (https://www.ncbi.nlm.nih.gov/genbank/). The accession numbers are provided as Table 1. Other datasets used and/or analyzed during the current study are available from the corresponding author on reasonable request.

Declarations

Ethics of approval and consent to participate

International ethical guidelines were followed to deal with the animals and the procedures were approved by the IACUC (Institutional Animal Care and Use Committee) at Hunter Biotechnology, Inc. and the IACUC approval number was 001458. The zebrafish facility and the laboratory at Hunter Biotechnology, Inc. are accredited by the Association for Assessment and Accreditation of Laboratory Animal Care (AAALAC) International.

Consent for publication

Not applicable.

Competing interests

The authors declare that they have no competing interests.

Author details

[1]Fisheries Research Institute of Fujian, Key Laboratory of Cultivation and High-value Utilization of Marine Organisms in Fujian Province, No. 7, Haishan Road, Huli District, Xiamen 361013, Fujian, China. [2]School of Life Sciences, Xiamen University, South Xiangan Road, Xiang'an District, Xiamen 361102, Fujian, China. [3]School of Environmental Science and Engineering, Southern University of Science and Technology, Shenzhen 518055, Guangdong, China. [4]College of the Environment and Ecology, Xiamen University, Xiamen 361102, Fujian, China. [5]Xiamen Medical College, Xiamen 361023, Fujian, China.

Received: 4 August 2021 Accepted: 25 April 2022
Published online: 21 May 2022

References

1. Dare RG, Oliveira MM, Truiti MCT, Nakamura CV, Ximenes VF, Lautenschlager SOS. Abilities of protocatechuic acid and its alkyl esters, ethyl and heptyl protocatechuates, to counteract UVB-induced oxidative injuries and photoaging in fibroblasts L929 cell line. J Photochem Photobiol B. 2020;203:111771.
2. Liu W, Otkur W, Zhang Y, Li Q, Ye Y, Zang L, et al. Silibinin protects murine fibroblast L929 cells from UVB-induced apoptosis through the simultaneous inhibition of ATM-p53 pathway and autophagy. FEBS J. 2013;280(18):4572–84.
3. Heo SJ, Jeon YJ. Protective effect of fucoxanthin isolated from Sargassum siliquastrum on UV-B induced cell damage. J Photochem Photobiol B. 2009;95(2):101–7.
4. Martinez RM, Pinho-Ribeiro FA, Steffen VS, Caviglione CV, Vignoli JA, Barbosa DS, et al. Naringenin inhibits UVB irradiation-induced inflammation and oxidative stress in the skin of hairless mice. J Nat Prod. 2015;78(7):1647–55.
5. Chung KW, Choi YJ, Park MH, Jang EJ, Kim DH, Park BH, et al. Molecular insights into SIRT1 protection against UVB-induced skin fibroblast senescence by suppression of oxidative stress and p53 acetylation. J Gerontol A Biol Sci Med Sci. 2015;70(8):959–68.
6. Yuan Y, Zhang J, Fan J, Clark J, Shen P, Li Y, et al. Microwave assisted extraction of phenolic compounds from four economic brown macroalgae species and evaluation of their antioxidant activities and inhibitory effects on alpha-amylase, alpha-glucosidase, pancreatic lipase and tyrosinase. Food Res Int. 2018;113:288–97.

7. Aminina NM, Karaulova EP, Vishnevskaya TI, Yakush EV, Kim YK, Nam KH, et al. Characteristics of polyphenolic content in Brown algae of the Pacific coast of Russia. Molecules. 2020;25(17):3909-21.
8. Kim KC, Piao MJ, Zheng J, Yao CW, Cha JW, Kumara MH, et al. Fucodiphlorethol G purified from Ecklonia cava suppresses ultraviolet B radiation-induced oxidative stress and cellular damage. Biomol Ther (Seoul). 2014;22(4):301–7.
9. Vo TS, Kim SK, Ryu B, Ngo DH, Yoon NY, Bach LG, et al. The suppressive activity of Fucofuroeckol-a derived from Brown algal Ecklonia stolonifera Okamura on UVB-induced mast cell degranulation. Mar Drugs. 2018;16(1):1-9.
10. Heo SJ, Ko SC, Kang SM, Cha SH, Lee SH, Kang DH, et al. Inhibitory effect of diphlorethohydroxycarmalol on melanogenesis and its protective effect against UV-B radiation-induced cell damage. Food Chem Toxicol. 2010;48(5):1355–61.
11. Bao Y, He X, Wu W, Wang S, Dai J, Zhang Z, et al. Sulfated galactofucan from Sargassum thunbergii induces senescence in human lung cancer A549 cells. Food Funct. 2020;11(5):4785–92.
12. Ray RS, Agrawal N, Sharma A, Hans RK. Use of L-929 cell line for phototoxicity assessment. Toxicol in Vitro. 2008;22(7):1775–81.
13. Chen YH, Wen CC, Lin CY, Chou CY, Yang ZS, Wang YH. UV-induced fin damage in zebrafish as a system for evaluating the chemopreventive potential of broccoli and cauliflower extracts. Toxicol Mech Methods. 2011;21(1):63–9.
14. Chen Y, Chen Y, Chou C, Wen C, Cheng C. UV-protective activities of pineapple leaf extract in zebrafish embryos. Res Chem Intermed. 2019;45(1):65–75.
15. Singleton VL, Orthofer R, Lamuelaraventos RM. Analysis of total phenols and other oxidation substrates and antioxidants by means of folin-ciocalteu reagent. Methods Enzymol. 1999;299:152–78.
16. Yu D, Zhu H, Liu Y, Cao J, Zhang X. Regulation of proinflammatory cytokine expression in primary mouse astrocytes by coronavirus infection. J Virol. 2009;83(23):12204–14.
17. Wang Y, Wang L, Wen X, Hao D, Zhang N, He G, et al. NF-kappaB signaling in skin aging. Mech Ageing Dev. 2019;184:111160.
18. Kuo YH, Wu PY, Chen CW, Lin P, Wen KC, Lin CY, et al. N-(4-bromophenethyl) Caffeamide protects skin from UVB-induced inflammation through MAPK/IL-6/NF-kappaB-dependent signaling in human skin fibroblasts and hairless mouse skin. Molecules. 2017;22(10):1639-52.
19. Kim SY, Kim EA, Kim YS, Yu SK, Choi C, Lee JS, et al. Protective effects of polysaccharides from Psidium guajava leaves against oxidative stresses. Int J Biol Macromol. 2016;91:804–11.
20. Lee C, Park GH, Ahn EM, Park CI, Jang JH. Sargassum fulvellum protects HaCaT cells and BALB/c mice from UVB-induced Proinflammatory responses. Evid Based Complement Alternat Med. 2013;2013:747846.
21. Dare RG, Nakamura CV, Ximenes VF, Lautenschlager SOS. Tannic acid, a promising anti-photoaging agent: evidences of its antioxidant and anti-wrinkle potentials, and its ability to prevent photodamage and MMP-1 expression in L929 fibroblasts exposed to UVB. Free Radic Biol Med. 2020;160:342–55.
22. da Silva BTA, Peloi KE, Ximenes VF, Nakamura CV, de Oliveira Silva Lautenschlager S. 2-acetylphenothiazine protects L929 fibroblasts against UVB-induced oxidative damage. J Photochem Photobiol B. 2021;216:112130.
23. Ribeiro F, Martins V, Helito L-B, Danielle D, Vania C. The extended production of UV-induced reactive oxygen species in L929 fibroblasts is attenuated by posttreatment with Arrabidaea chica through scavenging mechanisms. J Photochem Photobiol B Biol. 2018;178:175–81.
24. Oliveira MM, Dare RG, Barizao EO, Visentainer JV, Romagnolo MB, Nakamura CV, et al. Photodamage attenuating potential of Nectandra hihua against UVB-induced oxidative stress in L929 fibroblasts. J Photochem Photobiol B. 2018;181:127–33.
25. Ryu HC, Kim C, Kim JY, Chung JH, Kim JH. UVB radiation induces apoptosis in keratinocytes by activating a pathway linked to "BLT2-reactive oxygen species". J Invest Dermatol. 2010;130(4):1095–106.
26. Zhu X, Li N, Wang Y, Ding L, Chen H, Yu Y, et al. Protective effects of quercetin on UVB irradiationinduced cytotoxicity through ROS clearance in keratinocyte cells. Oncol Rep. 2017;37(1):209–18.
27. Cruces E, Huovinen P, Gomez I. Phlorotannin and antioxidant responses upon short-term exposure to UV radiation and elevated temperature in three South Pacific kelps. Photochem Photobiol. 2012;88(1):58–66.
28. Booij-James IS, Dube SK, Jansen MA, Edelman M, Mattoo AK. Ultraviolet-B radiation impacts light-mediated turnover of the photosystem II reaction center heterodimer in Arabidopsis mutants altered in phenolic metabolism. Plant Physiol. 2000;124(3):1275–84.
29. Heo SJ, Ko SC, Cha SH, Kang DH, Park HS, Choi YU, et al. Effect of phlorotannins isolated from Ecklonia cava on melanogenesis and their protective effect against photo-oxidative stress induced by UV-B radiation. Toxicol in Vitro. 2009;23(6):1123–30.
30. Ko S, Cha S, Heo S, Lee S, Kang S, Jeon Y. Protective effect of Ecklonia cava on UVB-induced oxidative stress: in vitro and in vivo zebrafish model. J Appl Phycol. 2011;23(4):697–708.
31. Svobodova AR, Galandakova A, Sianska J, Dolezal D, Ulrichova J, Vostalova J. Acute exposure to solar simulated ultraviolet radiation affects oxidative stress-related biomarkers in skin, liver and blood of hairless mice. Biol Pharm Bull. 2011;34(4):471–9.
32. Jang J, Ye BR, Heo SJ, Oh C, Kang DH, Kim JH, et al. Photo-oxidative stress by ultraviolet-B radiation and antioxidative defense of eckstolonol in human keratinocytes. Environ Toxicol Pharmacol. 2012;34(3):926–34.
33. Piao MJ, Yoon WJ, Kang HK, Yoo ES, Koh YS, Kim DS, et al. Protective effect of the ethyl acetate fraction of Sargassum muticum against ultraviolet B-irradiated damage in human keratinocytes. Int J Mol Sci. 2011;12(11):8146–60.
34. Yin Y, Li W, Son YO, Sun L, Lu J, Kim D, et al. Quercitrin protects skin from UVB-induced oxidative damage. Toxicol Appl Pharmacol. 2013;269(2):89–99.
35. Yan Z, Zhong Y, Duan Y, Chen Q, Li F. Antioxidant mechanism of tea polyphenols and its impact on health benefits. Anim Nutr. 2020;6(2):115–23.
36. Jung KA, Kwak MK. The Nrf2 system as a potential target for the development of indirect antioxidants. Molecules. 2010;15(10):7266-91.
37. Joanna W, Amy P, Christopher S. Dissecting molecular cross-talk between Nrf2 and NF-κB response pathways. Biochem Soc Trans. 2015;43(4):621–6.
38. Li YW, Zhang Y, Zhang L, Li X, Yu JB, Zhang HT, et al. Protective effect of tea polyphenols on renal ischemia/reperfusion injury via suppressing the activation of TLR4/NF-kappaB p65 signal pathway. Gene. 2014;542(1):46–51.
39. Wang L, Lee W, Oh JY, Cui YR, Ryu B, Jeon YJ. Protective effect of sulfated polysaccharides from Celluclast-assisted extract of Hizikia fusiforme against ultraviolet B-induced skin damage by regulating NF-kappaB, AP-1, and MAPKs signaling pathways in vitro in human dermal fibroblasts. Mar Drugs. 2018;16(7):239-50.
40. Park SH, Lee SS, Bang MH, Jo SK, Jhee KH, Yang SA. Protection against UVB-induced damages in human dermal fibroblasts: efficacy of tricin isolated from enzyme-treated Zizania latifolia extract. Biosci Biotechnol Biochem. 2019;83(3):551–60.
41. Subedi L, Lee TH, Wahedi HM, Baek SH, Kim SY. Resveratrol-enriched Rice attenuates UVB-ROS-induced skin aging via downregulation of inflammatory cascades. Oxidative Med Cell Longev. 2017;2017:8379539.
42. Eom S, Lee EH, Park K, Kwon J, Kim P, Jung W, et al. Eckol from Eisenia bicyclis inhibits inflammation through the Akt/NF-κB signaling in Propionibacterium acnes-induced human keratinocyte Hacat cells. J Food Biochem. 2017;41(2):e12312.
43. Kang NJ, Koo DH, Kang GJ, Han SC, Lee BW, Koh YS, et al. Dieckol, a component of Ecklonia cava, suppresses the production of MDC/CCL22 via Down-regulating STAT1 pathway in interferon-gamma stimulated HaCaT human keratinocytes. Biomol Ther (Seoul). 2015;23(3):238–44.
44. Yang YI, Woo JH, Seo YJ, Lee KT, Lim Y, Choi JH. Protective effect of Brown alga Phlorotannins against hyper-inflammatory responses in lipopolysaccharide-induced Sepsis models. J Agric Food Chem. 2016;64(3):570–8.
45. Lee SH, Eom S, Yoon N, Kim M, Li Y, Ha SK, et al. Fucofuroeckol-a from Eisenia bicyclis inhibits inflammation in lipopolysaccharide-induced mouse macrophages via downregulation of the MAPK/NF-κB signaling pathway. J Chem. 2016;2016(2016):1–9.
46. Yang YI, Jung SH, Lee KT, Choi JH. 8,8′-Bieckol, isolated from edible brown algae, exerts its anti-inflammatory effects through inhibition of NF-kappaB signaling and ROS production in LPS-stimulated macrophages. Int Immunopharmacol. 2014;23(2):460–8.
47. Wang L, Kim HS, Oh JY, Je JG, Jeon YJ, Ryu B. Protective effect of diphlorethohydroxycarmalol isolated from Ishige okamurae against UVB-induced damagein vitro in human dermal fibroblasts and in vivo in zebrafish. Food Chem Toxicol. 2020;136:110963.

48. Cha SH, Ko CI, Kim D, Jeon YJ. Protective effects of phlorotannins against ultraviolet B radiation in zebrafish (Danio rerio). Vet Dermatol. 2012;23(1):51–6, e12.
49. Wang L, Ryu B, Kim W, Kim GH, Jeon Y. Protective effect of gallic acid derivatives from the freshwater green alga Spirogyra sp. against ultraviolet B-induced apoptosis through reactive oxygen species clearance in human keratinocytes and zebrafish. Algae. 2017;32(4):379–88.
50. Guinea M, Franco V, Araujo-Bazan L, Rodriguez-Martin I, Gonzalez S. In vivo UVB-photoprotective activity of extracts from commercial marine macroalgae. Food Chem Toxicol. 2012;50(3–4):1109–17.
51. Muzaffer U, Paul VI, Prasad NR, Karthikeyan R. Juglans regia L. protects against UVB induced apoptosis in human epidermal keratinocytes. Biochem Biophys Rep. 2018;13:109–15.
52. Ryu B, Ahn BN, Kang KH, Kim YS, Li YX, Kong CS, et al. Dioxinodehydroeckol protects human keratinocyte cells from UVB-induced apoptosis modulated by related genes Bax/Bcl-2 and caspase pathway. J Photochem Photobiol B. 2015;153:352–7.
53. Piao MJ, Lee NH, Chae S, Hyun JW. Eckol inhibits ultraviolet B-induced cell damage in human keratinocytes via a decrease in oxidative stress. Biol Pharm Bull. 2012;35(6):873–80.
54. Piao MJ, Zhang R, Lee NH, Hyun JW. Protective effect of triphlorethol-a against ultraviolet B-mediated damage of human keratinocytes. J Photochem Photobiol B. 2012;106:74–80.
55. Seok JK, Boo YC. P-Coumaric acid attenuates UVB-induced release of Stratifin from keratinocytes and indirectly regulates matrix metalloproteinase 1 release from fibroblasts. Korean J Physiol Pharmacol. 2015;19(3):241–7.
56. Lee EH, Park HJ, Kim HH, Jung HY, Kang IK, Cho YJ. Isolated isoquercitrin from green ball apple peel inhibits photoaging in CCD-986Sk fibroblasts cells via modulation of the MMPs signaling. J Cosmet Dermatol. 2021;20(9):2932–9.
57. Hwang E, Park SY, Lee HJ, Lee TY, Sun ZW, Yi TH. Gallic acid regulates skin photoaging in UVB-exposed fibroblast and hairless mice. Phytother Res. 2014;28(12):1778–88.

Publisher's Note